Journal of Fluorine Chemistry 131 (2010) 1327–1337

Contents lists available at ScienceDirect

Journal of Fluorine Chemistry

journal homepage: www.elsevier.com/locate/fluor

Regiospecific nucleophilic substitution in 2,3,4,5,6-pentafluorobiphenyl as model compound for supramolecular systems. Theoretical study of transition states and energy profiles, evidence for tetrahedral S_N2 mechanism

Jaroslav Kvíčala [a,1], Michal Beneš [a,1], Oldřich Paleta [a,*], Vladimír Král [b]

[a] Department of Organic Chemistry, Institute of Chemical Technology Prague, Technická 5, Ustav organicke chemie Technicka, 16628 Prague 6, Czech Republic
[b] Department of Analytical Chemistry, Institute of Chemical Technology Prague, Technická 5, 16628 Prague 6, Czech Republic

ARTICLE INFO

Article history:
Received 18 June 2010
Received in revised form 8 September 2010
Accepted 15 September 2010
Available online 22 September 2010

Keywords:
2,3,4,5,6-Pentafluorobiphenyl
meso-5,10,15,20-Tetrakis-(pentafluorophenyl)-porphyrin
Nucleophilic substitution
Computational chemistry
Meisenheimer complex
Tetrahedral S_N2 mechanism

ABSTRACT

2,3,4,5,6-Pentafluorobiphenyl (PFBi) was modified by the nucleophilic substitution of one fluorine using a series of O-, S- and N-nucleophiles, viz. alkaline salts of 2,2,2-trifluoro-ethanol, 3,3,4,4,5,5,6,6,7,7,8,8,8-tridecafluorooctanol, 1,2;3,4-di-O-isopropylidenexylitol, allylsulfane, 3,3,4,4,5,5,6,6,7,7,8,8,8-tridecafluorooctane-1-thiol, 3-aminopropan-1-ol (**7**), and tert-butyl N-(3-aminopropyl)carbamate (**8**). All the substitutions took place exclusively at the position para to the phenyl group. (3-Amino-propyl)amino derivative of PFBi (**15**) was further modified at the terminal amino group by acylation or fluoroalkylation. The reaction of **8** was applied to *meso*-5,10,15,20-tetrakis-(pentafluorophenyl)porphyrin (**20**) to afford tris- (**21**) and tetrakis-substituted (**22**) products with complete para-regioselectivity. Theoretical studies of the reaction pathways of PFBi with ammonia, microsolvated lithium fluoride or lithium hydroxide revealed that no Meisenheimer-type intermediates are formed in the course of the simulated reactions: instead, tetrahedral S_N2 mechanism was found. Significant regioselectivity of the nucleophilic aromatic substitution, leading to 4-substituted products, was predicted based on relative transition state energies in agreement with the observed experimental results.

1. Introduction

Pentafluorophenyl group easily undergoes nucleophilic replacement of fluorine, e.g. in 2,3,4,5,6-pentafluorobenzonitrile [1], 2,3,4,5,6-pentafluorotoluene [2,3] or 2,3,4,5,6-pentafluoro-biphenyl [3a,4,5]. This group can be introduced to particular molecules as macrocycles or other supermolecules and nanostructures to enable their further modification at the peripheral parts. Typical examples have been substituted porphyrins or metalloporphyrins bearing *meso*-penta-fluorophenyl groups, in which the pentafluorophenyl moieties were modified by aromatic nucleophilic replacement [6–9].

Explorational experiments with macrocyclic compounds are usually expensive owing to high prices of the substrates. Therefore, we were looking for a commercially accessible model compound for *meso*-pentafluorophenylated porphyrin that would reflect its chemical properties as much as possible. Such compound has been found in 2,3,4,5,6-pentafluorobiphenyl (PFBi, **1a**). We have verified on 5,10,15,20-tetrakis(pentafluorophenyl)-porphyrin that PFBi could well simulate chemical properties of this macrocycle [8]. In this paper we present regiospecific aromatic nucleophilic substitutions of fluorine in PFBi, which have been successfully applied in particular cases to the pentafluorophenylated porphyrin [8].

The second advantage of PFBi as a model compound has been the complete regioselectivity of nucleophilic displacements of fluorine atom in this substrate. The nucleophilic reactions on PFBi reported so far, viz. reactions with O- [3a,4], S- [5a] or N-nucleophiles [5] took place exclusively at the *para*-position with respect to the phenyl group in PFBi. The same regioselectivity has been observed for 5,10,15,20-tetrakis(pentafluorophenyl)porphyrin [6–9].

2. Experimental results and discussion

An overview of the nucleophilic substitutions in PFBi studied in this work is given in Table 1 together with the structures of the products **9**–**15**. All the substitutions took place with the complete regioselectivity and exclusive nucleophilic attack at the position *para* with respect to the phenyl group. No byproducts were formed in the reactions as verified by checking the reaction mixtures by ^{19}F NMR or following the reactions by ^{19}F NMR.

2.1. Reactions of pentafluorobiphenyl with O-nucleophiles

O-Nucleophiles used were alkoxides of the mother hydroxy compounds, because free hydroxyls appeared to react very slowly.

* Corresponding author. Fax: +420 224311082/220444288.
E-mail addresses: Jaroslav.Kvicala@vscht.cz (J. Kvíčala), Oldrich.Paleta@vscht.cz (O. Paleta).
[1] Fax: +420 220 444288.

0022-1139/$ – see front matter © 2010 Elsevier B.V. All rights reserved.
doi:10.1016/j.jfluchem.2010.09.003

Table 1
Overview of nucleophilic substitution reactions.

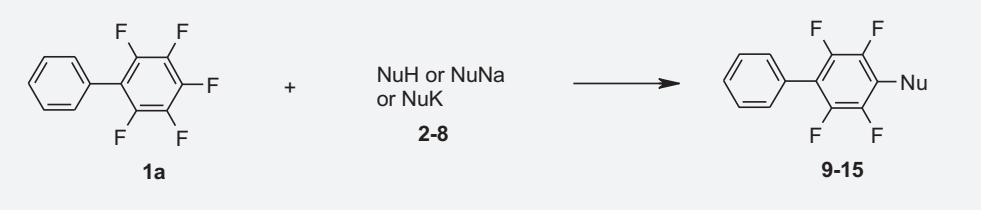

.

Entry no.	Nucleophile	Product	Yield (%)
1	**2**	CF_3-CH_2-OH + K_2CO_3	**9**	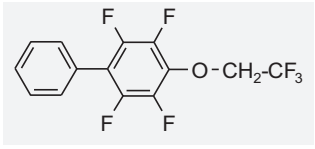	97
2	**3**	CF_3-$(CF_2)_4$-CF_2-CH_2-CH_2-ONa	**10**	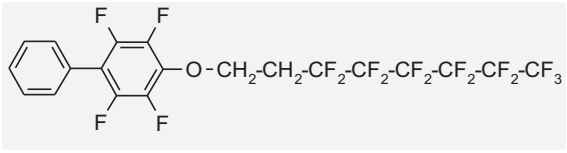	38
3	**4**	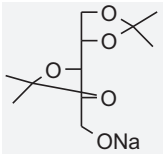	**11**	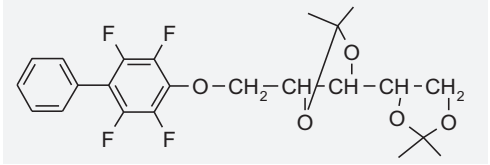	60
4	**5**	CH_2=CH-CH_2-SH + K_2CO_3	**12**	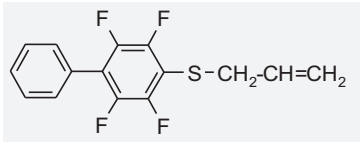	96
5	**6**	CF_3-$(CF_2)_6$-CF_2-CH_2-CH_2-SH + K_2CO_3	**13**	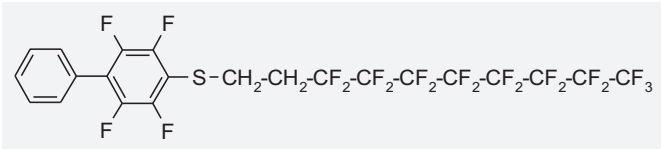	92
6	**7**	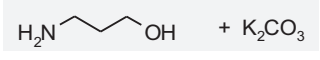	**14**	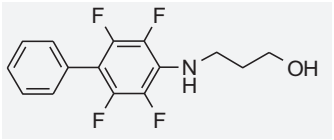	60
7	**8**	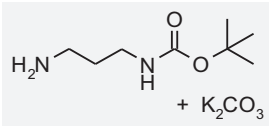	**15**	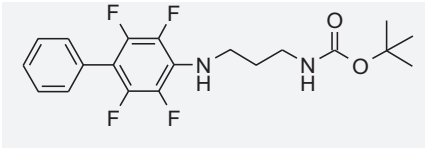	74

In the case of 2,2,2-trifluoroethanol (**2**), the corresponding alkoxylate was generated directly in the reaction mixture using potassium carbonate in refluxing dioxane to give the desired ether **9** in 97% yield in 3 days. Nucleophilic alkoxides of 2-(perfluorohexyl)ethan-1-ol (**3**) and 1,2;3,4-di-*O*-isopropylidene-D-xylitol (**4**) were prepared by their reaction with sodium hydride in tetrahydrofuran and afforded the corresponding substitution products **10** (38%) and **11** (60%), respectively.

2.2. Reactions of pentafluorobiphenyl with S- and N-nucleophiles

PFBi (**1a**) reacted very easily with *S*-nucleophiles. The substitution reactions were carried out in *N*,*N*-dimethylformamide in the presence of potassium carbonate at 40–50 °C. Allyl thiol (**5**) afforded the sulfide **12** in a 96% isolated yield, while in the reaction of 2-(perfluoroctyl)ethane-1-thiol (**6**) the resulting sulfide **13** was obtained in a 92% isolated yield.

The reactions of primary amines with PFBi were performed in the presence of potassium carbonate. 3-Aminopropanol (**7**) was used in an unprotected form as the amino group appeared to be much more reactive than the hydroxy group. The reaction in refluxing dioxane was rather slow and afforded the expected substitution product **14** in 60% yield in 3 weeks. The reaction proceeded more rapidly in *N*,*N*-dimethylformamide at 50 °C to afford the product **14** in 40% isolated yield in 5 days. Propane-1,3-diamine was used in BOC-semiprotected form **8** and the reaction in refluxing dioxane gave the expected product **15** in 74% yield. No byproducts were detected in the above reactions.

2.3. Transformations of substitution products and porphyrin derivatives

The sulfide **13** was subsequently oxidized by trifluoroperoxyacetic acid to the corresponding and more hydrophilic sulfoxide **16** in 82% yield (Scheme 1). The successful preparation of the diamine derivative **15** offered a possibility for further transformations of the terminal amino group by fluoroacylation and fluoroalkylation reactions (Scheme 1). First, the amino group was deprotected in aprotic acid media [10] to give hydrochloride **17** (yield 98%). Its reaction with triethylamine in dichloromethane liberated free amine, which was *in situ* acylated by perfluorooctanoyl chloride to afford the compound **18** in 72% isolated yield. Fluoroalkylation of the hydrochloride **17** was carried out using 2-(2,2,3,3,4,4,5,5,6,6,7,7-tridecafluoroheptyl)-oxirane [11] in the presence of triethylamine. The reaction in 2,2,2-trifluoroethanol at 60 °C gave bis-hydroxyfluoroalkylated derivative **19** in 49% yield.

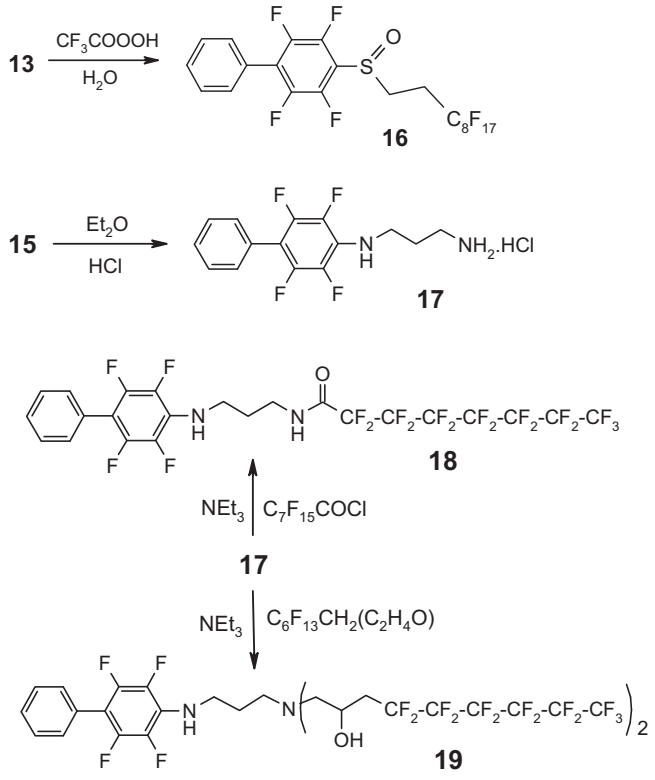

Scheme 1. Transformations of the products of primary substitution in PFBi.

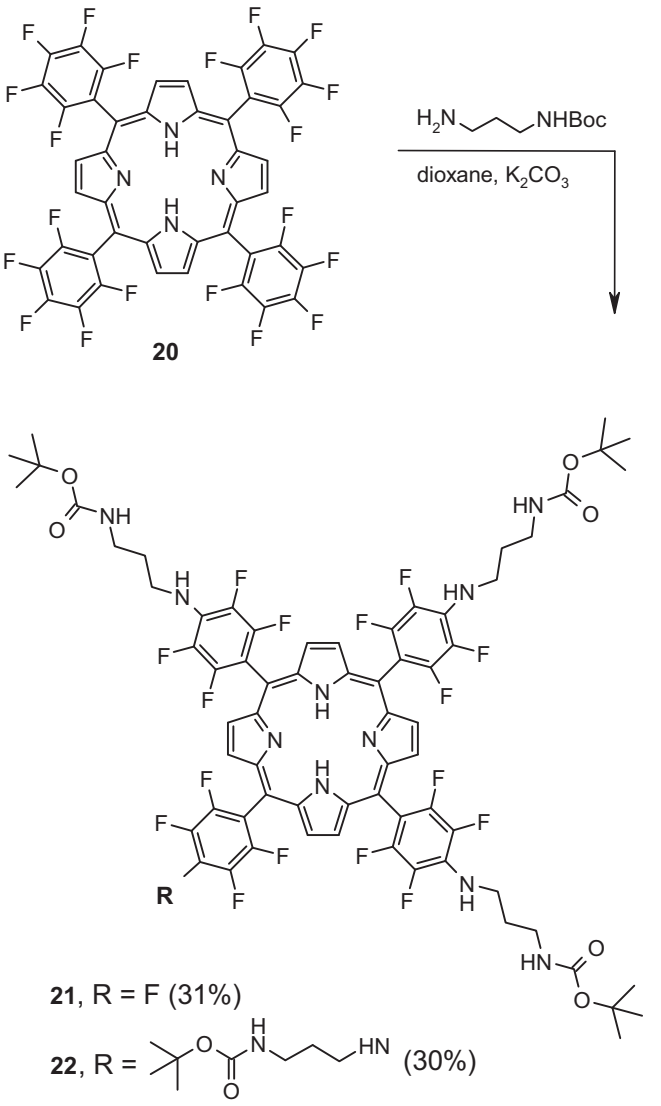

Scheme 2. Alkylaminations in *meso*-5,10,15,20-tetrakis(pentafluorophenyl)porphyrin (**20**).

Our experience in the chemistry denoted in Table 1 has been applied to *meso*-5,10,15,20-tetrakis(pentafluorophenyl)porphyrin (**20**) as reported in our recent papers [8]. In this paper, the reaction of **20** with Boc-semiprotected propane-1,3-diamine (**8**, Scheme 2) in dioxane at 100 °C was studied: it proceeded slowly and even after three weeks the monosubstitution of fluorine atoms in pentafluorophenyls was not complete to afford a mixture of tris- (**21**) and tetrakis-substituted (**22**) products in 31% and 30% respective yields.

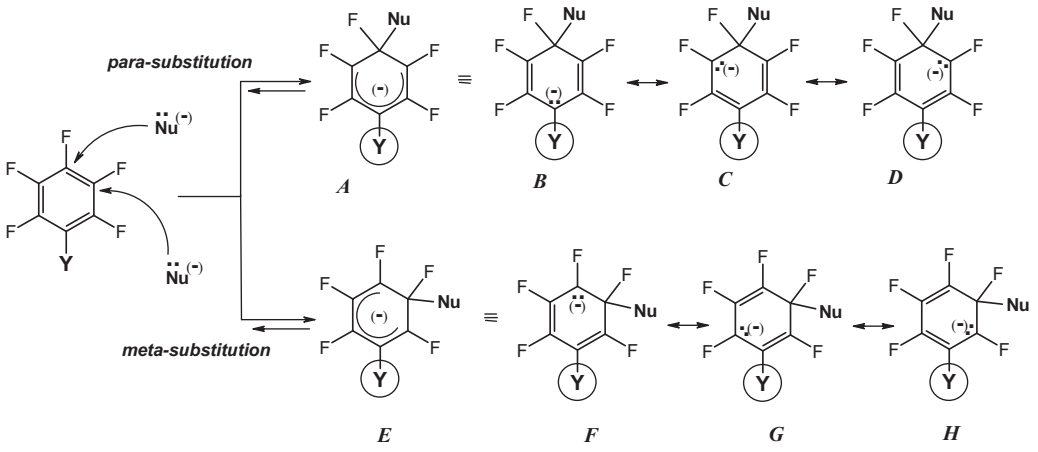

Y = C_6H_5 (**1a**), H (**1b**), F (**1c**), CH_3 (**1d**), OCH_3 (**1e**), NH_2 (**1f**)

Scheme 3. Regioselectivity of nucleophilic substitution of fluorine in monosubstituted pentafluorobenzene moiety.

2.4. Regioselectivity of the substitutions in terms of substituent effects and mesomeric concept

PFbi (**1a**) can be considered as one member of the series of substituted pentafluorobenzenes having a general structure **1** with a substituent Y (Scheme 3). The results of the regioselectivity of nucleophilic substitutions in the compounds **1a**–**1f** are summarised in Table 2. The data reveal that *para*- and/or *meta*- and *ortho*-substitution occur in dependence on the character of the substituent Y. Substituents attached to an aromatic system are characterised by the Hammett σ_p substitutent constants. The values of the Hammett σ_p constants in Table 2 exhibit that substituents OCH_3 and NH_2 having negative value of σ_p below −0.20 cause *meta*-substitution. Schematic transition states (activated complexes) for *para*- and *meta*-substitution, which may not be Meisenheimer-type intermediates, are illustrated by the structures **A** and **E** in Scheme 3.

An explanation of the *para*- (and *ortho*-) or *meta*-substitution using the Hammett constants can be interpreted by the mesomeric concept as an adequate theoretical background. Negative values of the quantities σ_p mean destabilisation of a negative charge. For the *para*-substitution, the mesomeric (resonance) structures **B**–**D** can be drawn (Scheme 3). In the structure **B**, the substituent Y interacts with an alpha-negative charge, which is stabilised by substituents with positive σ_p value. The more negative value of a σ_p constant, the higher destabilisation of the mesomeric structure **B**. An analogous set of mesomeric structures can be drawn for the *ortho*-substitution. Fluorine substituents in the C_6F_5 moiety are also active from the mesomeric point of view and support of a nucleophilic substitution [12], but the system is the same for all the substituents discussed.

On the other hand, in the mesomeric (resonance) structures **F**–**H** for the *meta*-substitution the substituent Y does not interact with the alpha-negative charge. For that reason, the set **F**–**H** is more stable (less energetic) for substituents Y with a (higher) negative value of the σ_p constant than the set **B**–**D**. The result is that in the compounds **1e** or **1f** (Table 2) the substituents OCH_3 or NH_2 support *meta*-substitution. A small portion of the *ortho*-substitution in **1b** and **1e** can be combined with a smaller steric effect of the substituents H and OCH_3 relatively to CH_3, NH_2 and C_6H_5 [13], which block the access of a nucleophilic reagent to the *ortho*-position.

Table 2
Regioselectivity of the S_N reactions according the Scheme 3 and Hammett σ_p constants.

	Y	Regioselectivity of S_N	Ref.	Hammett[a] σ_p const.
1a	C_6H_5	*para*	[3a,4,5]	0.02
1b	H	*para* (95–97%) + *ortho* (3–5%)	[14]	0.00
1c	F	S_N	[15b,c]	0.06
1d	CH_3	*para*	[2,3]	−0.14
1e	OCH_3	*para* (52%) + *ortho* (16%) + *meta* (36%)	[15a]	−0.28
1f	NH_2	*meta* (79–90%) + *para* (10–21%)	[12,16]	−0.57

[a] Ref. [13].

3. Quantum chemical calculations of the reaction of 2,3,4,5,6-pentafluorobiphenyl (1*a*) with model nucleophiles

Excluding early semiempirical studies, only a few papers can be found dealing with computations on nucleophilic aromatic substitution at *ab initio* or DFT levels. Thus, for the model reactions of monohaloarenes with halide anions the attack of fluoride on fluorobenzenes proceeds through Meisenheimer complex. Moreover, this complex is a global minimum on the PES (potential energy surface). In contrast to that, no such complex was found for other halobenzene-halide systems [17]. Simulated reaction of pentafluoronitrobenzene with ammonia proceeded through the corresponding intermediary Meisenheimer complex as a shallow minimum for *ortho* substitution, however, no such intermediate was found for the *para* attack [18]. In contrast to this, simulated reactions of a series of perfluoroarenes including perfluorobiphenyl with naked fluoride ion gave Meisenheimer complexes which corresponded well with experimentally observed sites of attack [19]. No transition states were reported in this paper.

3.1. Calculations with ammonia as a model nitrogen nucleophile

Strong preference for the substitution of PFBi (1a) with nucleophiles at the position 4 was observed experimentally. To understand better the reasons for the high regioselectivity, we decided to study computationally aromatic nucleophilic substitution on PFBi. As a first model nucleophile, we chose ammonia as the simplest nitrogen nucleophile and as the respective centres of nucleophilic attack C-3 and C-4 carbons of the PFBi (**1a**) skeleton. Our computational study started with geometry optimization of

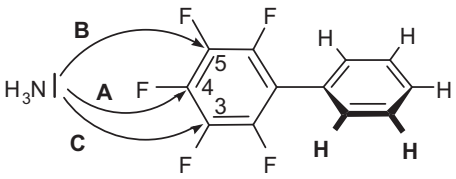

Fig. 1. Considered nucleophilic attacks of ammonia on PFBi (**1a**): due to the C_2 symmetry of the substrate, front face and rear face attacks of ammonia on C(4) are equivalent (path A), while front face attack on C(5) is equivalent with rear face attack on C(3) (path B) and front face attack on C(3) is equivalent with rear face attack on C(5) path (C).

PFBi. The calculated torsion angle between both aromatic rings is 46° as a result of compromise between attempts to preserve at least some aromaticity and steric hindrance of the *ortho*-substituents in good agreement with a 53° angle found in the crystal structure [20]. Following that, three nucleophilic attacks were considered in the calculations, i.e. pathways A (at C-4), B (at less hindered *meta* side denoted here C-5) and C (at more hindered *meta* side denoted C-3) (Fig. 1).

The reaction pathway study started with finding equilibrium geometries. We employed DFT method at the PBE1PBE/6-31+G(d) level of theory (Fig. 2, Table 3). We generally prefer PBE1PBE hybrid functional over the common B3LYP functional, as the former contains only one non-empirical parameter (hence this functional is also named PBE0) and has better description of systems with non-covalent interactions [21]. Due to the formation of fluoride anion in the course of the reaction, we also included a single set of diffuse functions into the basis set used to achieve correct description of anionic intermediates.

Search for saddle points revealed in analogy to Ref. [18] no intermediary Meisenheimer complexes on the PES, the corresponding Meisenheimer structures being transition states as confirmed by vibrational analysis. IRC calculations of both sides of all three reaction pathways A–C (Fig. 2) starting from the corresponding transition states did not find any intermediary local minima between the depicted transition states and educts/products clusters (Fig. 2).

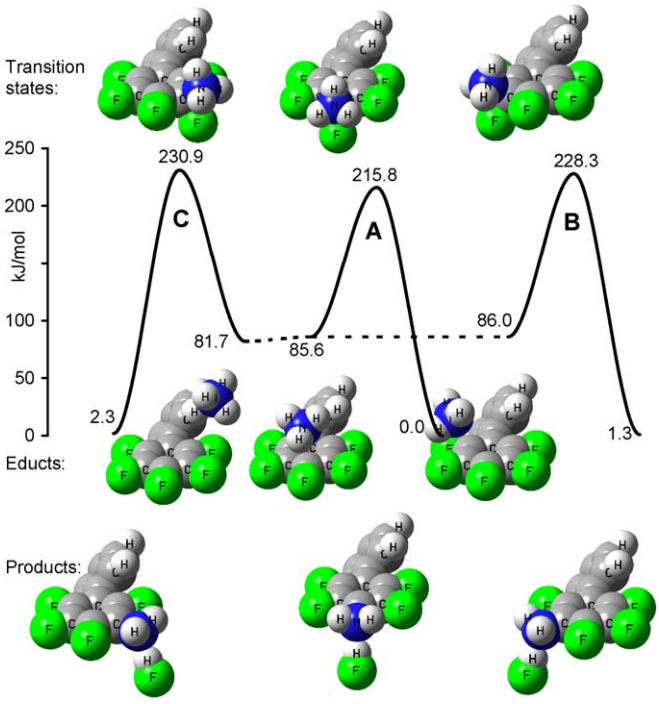

Fig. 2. Energies and structures of saddle points of the reaction of pentafluorobiphenyl (**1a**) with ammonia (PBE1PBE/6-31+G(d)).

We did not find any minimum with ammonia complexed to the pentafluorobiphenyl molecule (**1a**) at the C-3 for pathway C due to preferred coordination of ammonia to *ortho*-hydrogen of the pentafluorobiphenyl system, which leads to a local minimum lower by ca. 4 kJ mol^{-1} than other precoordinated educts.

Inspection of all three reaction pathways A–C proved that the reaction regioselectivity is driven kinetically as the barrier of the reverse reaction exceeds 200 kJ mol^{-1}, too high for making the reaction reversible under the experimental conditions compared to ca. 130 kJ mol^{-1} for the forward reaction. In agreement with the energies of published Meisenheimer intermediates [19], we found strong preference for the attack of ammonia at the C-4 position of

Table 3
Relative energies (kJ mol^{-1}) of educts, products and transition states of reaction of pentafluorobiphenyl (**1a**) with ammonia by various methods, role of inclusion of zero point energy (ZPE) and thermal correction (GFE, 298.15 K) into the calculations.

Method	Energy	Path C			Path A			Path B		
		Geometry			Geometry			Geometry		
		P	TS	E	E	TS	P	E	TS	P
I	$E_{rel.}$	2.3	230.9	81.7	85.6	215.8	0.0	86.0	228.3	1.3
	$E_{TSrel.}$		**15.1**			**0.0**			**12.5**	
II	$E_{rel.}$	2.4	250.3	82.8	85.7	234.5	0.0	86.3	247.8	1.4
	$E_{TSrel.}$		15.8			0.0			13.2	
III	$E_{rel.}$	3.5	310.0	60.4	60.8	292.7	0.0	61.3	307.7	2.7
	$E_{TSrel.}$		15.0			0.0			17.3	
IV	$E_{rel.}$	2.6	255.9	76.9	78.4	240.0	0.0	79.1	253.5	1.5
	$E_{TSrel.}$		15.9			0.0			13.6	
V	$E_{rel.}$	2.8	230.3	99.2	100.9	209.1	0.0	101.3	228.3	2.4
	$E_{TSrel.}$		**21.2**			**0.0**			**19.2**	
I	$E_{rel.}$	2.3	232.2	76.9	79.2	219.4	0.0	79.5	229.7	1.4
E+ZPE	$E_{TSrel.}$		12.8			0.0			10.3	
I	$E_{rel.}$	2.5	240.2	70.3	64.0	227.1	0.0	69.5	237.8	1.8
GFE	$E_{TSrel.}$		**13.0**			**0.0**			**10.7**	
V	$E_{rel.}$	1.6	227.2	95.9	94.3	207.9	0.0	94.7	224.9	3.6
E+ZPE	$E_{TSrel.}$		19.3			0.0			17.0	
V	$E_{rel.}$	0.4	234.4	91.9	92.1	214.7	0.0	97.0	231.8	5.5
GFE	$E_{TSrel.}$		**19.7**			**0.0**			**17.1**	

A: C-4 substitution; B: C-5 substitution (less hindered); C: C-3 substitution (more hindered); P: products; TS: transition state; E: educts; I: PBE1PBE/6-31+G(d)//PBE1PBE/6-31+G(d); II: PBE1PBE/6-311++ G(2df,p)//PBE1PBE/6-31+G(d); III: MP2/6-311++G(2df,p)//PBE1PBE/6-31+G(d); IV: BMK/6-311++G(2df,p)//PBE1PBE/6-31+G(d); V IEFPCM(THF)BMK/6-311++G(2df,p)//IEFPCM(THF)-BMK/6-311++G (2df,p); E: electronic energy; E+ZPE: electronic energy + zero point energy; GFE: Gibbs free energy.

PFBi, the difference in the transition state energy being ca. 12 kJ mol^{-1}, which corresponds to more than 99% excess of the *para*-substituted product (Table 3).

3.2. Role of computational method, ZPE and thermochemical correction

To evaluate a quality of the correlation description we recalculated the energies of all saddle points in the A–C (Fig. 2) pathways using three various approaches. First, we employed the same PBE1PBE functional with larger triple zeta basis set and more polarization functions (PBE1PBE/6-311++G(2df,p)), and then compared the results from DFT method with those obtained by simple perturbation treatment (MP2/6-311++G(2df,p)). Further we recalculated the energies using the BMK functional (BMK/6-311++G(2df,p)), which is especially tailored for the transition state calculations and gives results comparable or better than much more demanding multiconfigurational methods [22]. Finally, as the reactions were performed mostly in THF, we reoptimized all saddle points using the BMK/6-311++G(2df,p) method in a simulated solvent using an IEF-PCM approach [23]. Although the actual values of the activation energies change with the method employed, the relative energies of the transition states for the pathways A–C vary only by a few kJ mol^{-1}. Thus, using a larger basis set in the PBE1PBE method enhances a little the absolute values of the transition state energies, MP2 method probably overestimates the transition state energies and BMK method affords values higher than other DFT methods but lower than MP2. Inclusion of the solvent effects reduces the absolute values of the transition state energies to the levels of the simplest method used (PBE1PBE/6-31+G(d)), but results in even higher preference for C-4 substitution. In all cases, the relative energy of the transition state of the A pathway is at least 10 kJ mol^{-1} smaller than the remaining two transition states energies implying more than 98% excess of the C-4 substituted product. The best method employed rises the transition state energy to more than 19 kJ mol^{-1} (Table 4, Fig. 1 in Supporting info). Finally, we compared for both optimization method used, (PBE1PBE/6-31+G(d) and IEFPCM(THF)-BMK/6-311++G (2df,p)), pure electronic energies, electronic energies including zero point energy (ZPE) and Gibbs free energies (GFE). The results show that considering the ZPE lowered the corresponding relative energy barriers of pathways B and C (Fig. 2) by about 2 kJ mol^{-1} for both methods used, while the correction to room temperature and other thermochemical parameters (vibration, rotation, translation, entropy) did not change these values significantly (see Table 4).

3.3. Calculations with microsolvated fluoride ion

For the model reactions with fluoride ion, to obtain results comparable with the most recent published data [19] we started this part of computational study by the search for saddle points of the reaction of decafluorobiphenyl with naked fluoride anion. We indeed obtained using our level of theory (PBE1PBE/6-31+G(d)) comparable results with global minimum being the corresponding Meisenheimer complex of the C-4 substitution and local minimum its analogue for the C-3 substitution. However, apart of the Meisenheimer complexes, no other minima on the potential energy surface (PES) of the system, as well as no transition states corresponding to the formation of these complexes could be found (see Supporting info). Similar results, i.e. preference for the C-4 attack over other positions and non-existence of other saddle points other than that between the Meisenheimer complexes were obtained for simulated reaction of naked fluoride ion with PFBi (**1a**).

To our opinion, these results indicate that the use of naked fluoride anion for calculations of simulated aromatic nucleophilic substitution leads to completely incorrect description of PES of the studied system. Especially, naked fluoride anion displays too high reactivity and hence neither the fluoride ion-fluoroarene cluster, not the transition state between this structure and Meisenheimer complex could be detected. In agreement with this, fluoride ion in ethereal solvents exist mostly as a tight ion pair with the corresponding cation. We hence decided to add lithium cation to the fluoride anion to complete the modified nucleophile. Moreover, due to characteristic tetracoordination of lithium cation, we included microsolvation to it in the form of two dimethyl ether molecules. The respective fourth coordination site of the lithium cation was implied to be occupied by the substrate.

In contrast to the computations including naked fluoride ion, search for saddle points of the reaction of PFBi in analogy to the ammonia–PFBi system using modified nucleophile–2DME-LiF, proceeded smoothly. First, both precomplexed educt clusters and the complexed product clusters were found quite easily, second, no Meisenheimer complexes were detected on the PES, the corresponding structures being the transition states (Fig. 3, Table 5). The reaction pathways were again checked by IRC calculations for the presence of local minima (Fig. 3, Table 4). As the nucleophile and leaving group are identical in this case, the simulated reaction pathway of the C-4 attack is symmetrical. Moreover, the forward reaction of microsolvated fluoride ion at C-3 is identical with the reverse reaction at C-5 and, correspondingly, only two reaction pathways were studied. Similarly to the ammonia as the model nucleophile, we were not able to find the minimum corresponding to the educt-substrate cluster for the C-3 attack due to preferable coordination of the nucleophile to the *ortho*-hydrogen of the phenyl group.

Table 4
Relative energies (kJ mol^{-1}) of educts, products and transition states of reaction of pentafluorobiphenyl (**1a**) with 2DME-LiF cluster at the PBE1PBE/6-31+G(d) level of theory.

Energy	Path A			Path B		
	Geometry			Geometry		
	E	TS	P	E	TS	P
$E_{rel.}$	8.5	93.7	8.5	8.5	107.1	0.0
$E_{TSrel.}$		**0.0**			**13.4**	

A: C-4 substitution; B: C-5 substitution (less hindered). P: products; TS: transition state; E: educts.

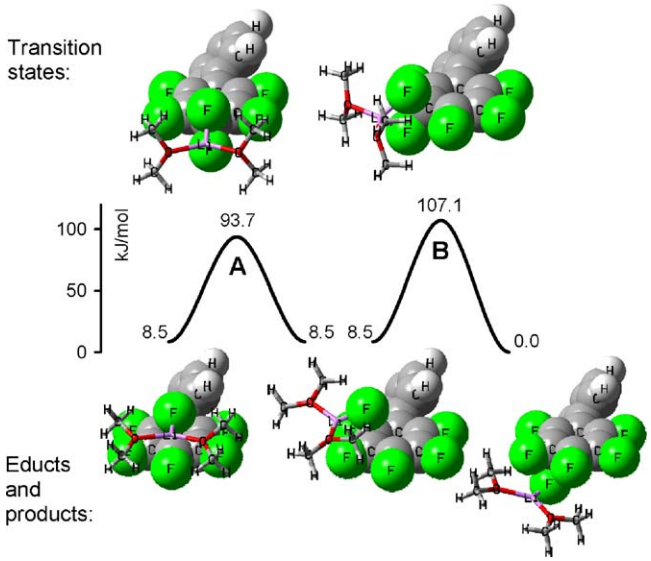

Fig. 3. Energies and structures of saddle points of reaction of pentafluorobiphenyl (**1a**) with 2DME-LiF cluster (PBE1PBE/6-31+G(d)).

Table 5
Relative energies (kJ mol^{-1}) of educts, products and transition states of reaction of pentafluorobiphenyl (**1a**) with 2DME-LiOH cluster at the PBE1PBE/6-31+G(d) level of theory.

Energy	Path C			Path A			Path B		
	Geometry			Geometry			Geometry		
	P	TS	E	E	TS	P	E	TS	P
$E_{rel.}$	17.3	189.5	144.5	153.6	177.3	14.2	154.1	189.4	0.0
$E_{TSrel.}$		**12.2**			**0.0**			**12.0**	

A: C-4 substitution; B: C-5 substitution (less hindered); C: C-3 substitution (more hindered); P: products; TS: transition state; E: educts.

In analogy to the case of ammonia, substitution at C-4 proved to be energetically more favored with the corresponding transition state energy lower by more than 13 kJ mol^{-1} whereas no such preference could be observed for the educts cluster.

3.4. Calculations with microsolvated hydroxide ion

Following a successful description of the attack of the PFBi with fluoride anion, we used analogous approach for the reaction with hydroxide ion. Again, naked hydroxide anion is unrealistic in ethereal solvents used and its use in calculations led to the respective products at the C-3, C-4 and C-5 positions as the only saddle point which could be detected on the PES. However, addition of lithium microsolvated with two molecules of DME to the hydroxide anion led to the simulated nucleophile which allowed to identify educts clusters, transition states and products clusters as the respective saddle points on the PES (Fig. 4, Table 5).

Microsolvated hydroxide ion preserves high reactivity and hence the reactions proceed through early transition state with low activation energy. Transition state of the C-4 attack (pathway A) is again most favored by more than 12 kJ mol^{-1} in close analogy to both previously studied systems (NH_3, 2DME.LiF). Similarly to the previous systems, neither educts cluster of the C-3 attack nor products cluster of the C-5 attack could be found due to preferred coordination of the nucleophile to the *ortho*-hydrogen of the phenyl moiety. High activation energy of the reverse reaction (more than 160 kJ mol^{-1}) again indicates that the reaction is driven kinetically.

All equilibrium geometries (Cartesian coordinates) and their energies (hartree) are listed in Supporting information.

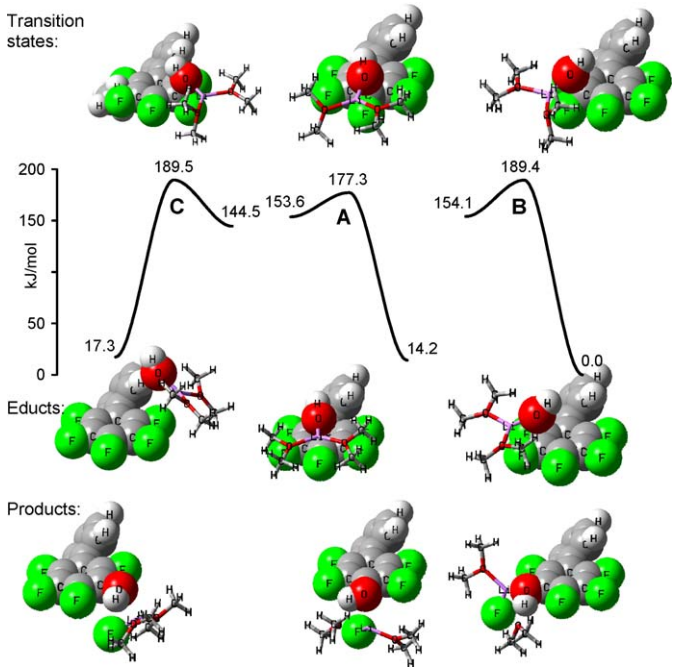

Fig. 4. Energies and structures of saddle points of reaction of pentafluorobiphenyl (**1a**) with 2DME-LiOH cluster (PBE1PBE/6-31+G(d)).

3.5. Attempted explanation of regioselectivity

Looking for the explanation of the high regioselectivity of nucleophilic aromatic substitution in PFBi, we turned our attention to two possible information sources, viz. analysis of charges on the individual reaction centres in the respective educt clusters and transition states, and analysis of frontier orbitals of the transition states.

Analysis of the atomic charges is not a simple issue in quantum chemistry and several approaches can be employed. As standard Mulliken atomic charges are generally regarded unreliable, we employed Merz–Singh–Kollman scheme based on ESP analysis [24]. In agreement with analysis of PFBi, no significant differences in atomic charges on the carbon centres in pentafluorophenyl part were found for the ammonia–PFBi educt clusters corresponding to pathways A–C (Figs. 2 and 5). However, this situation changed remarkably for the respective

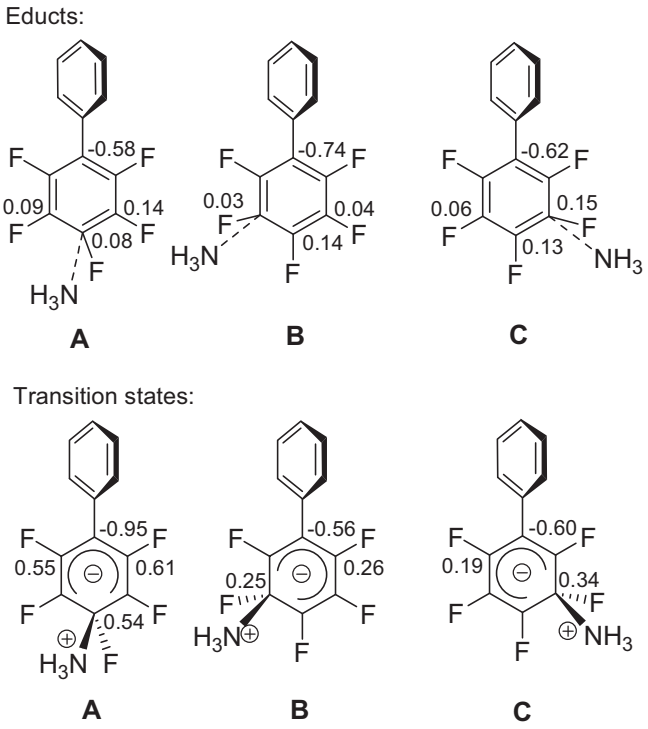

Fig. 5. Selected charges calculated according to the Merz–Singh–Kollman scheme for the ammonia–PFBi educt clusters and transition states corresponding to pathways A–C.

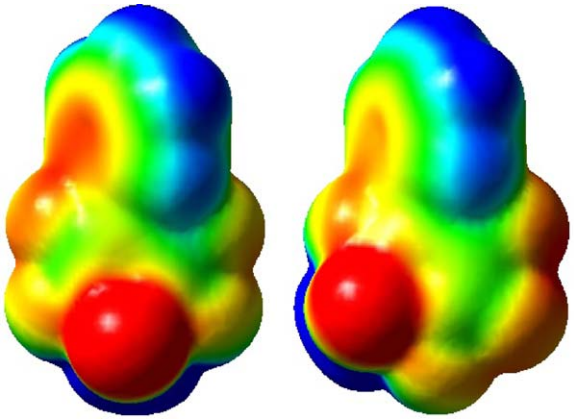

Fig. 6. Electrostatic potential mapped on isoelectronic surface for the ammonia–PFBi transition states corresponding to pathways A and C.

transition states. Thus, for the pathway A the charge on the attacked carbon C-4 reaches 0.54, while for the pathways B and C the values are 0.25 for C-5 and 0.34 for C-3. In agreement with this the charges on C-1 (phenyl substituted, which bears highest negative charge in educts) reach −0.95, −0.56 and −0.60 for the respective pathways A–C (Fig. 5). This indicates that for the most advantageous C-4 attack the π-electrons on the pentafluorophenyl ring are most polarizable facilitating the nucleophilic attack. The C-4 carbon of the PFBi (**1a**) seems to be the most prone to the dearomatization (the level of dearomatization can be estimated from the positive charge of the attacked carbon) and we assume that this is the major factor governing the regioselectivity.

Visualization of the electrostatic potential for transition states of pathways A and C (Fig. 6) revealed that some additional stabilization of the pathway A can be attributed by some electron flow to the partially conjugated phenyl ring.

Analysis of frontier orbitals revealed that the HOMO orbital of the C-4 attack transition state has significantly lower energy (by 0.007 hartree, i.e. 18 kJ mol^{-1}) than that of the C-3 attack, which corresponds well with the respective transition state energies. The HOMO of the transition state of the more favorable attack also spreads over the second aromatic ring in striking contrast to the other HOMO orbital (Fig. 7).

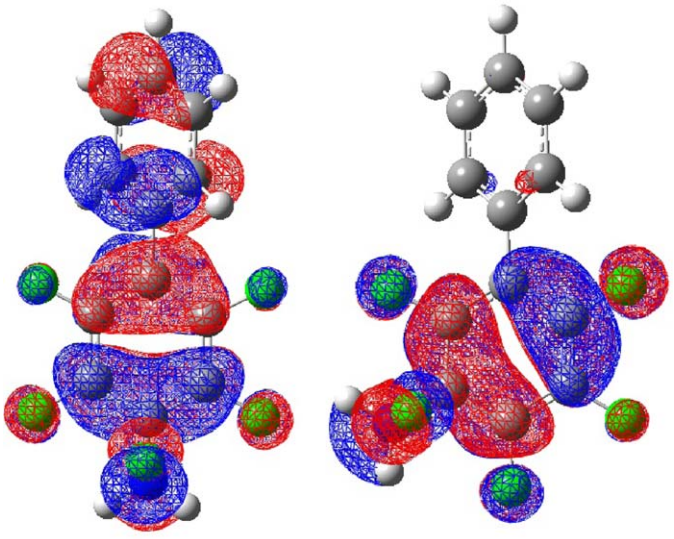

Fig. 7. HOMO orbitals of the ammonia-fluoroarene **1a** transition states.

4. Conclusions

Aromatic nucleophilic substitution reactions of PFBi (**1a**) with a series of (long-chain) fluorinated O-, S- and N-nucleophiles were studied as model reactions for supramolecular systems. The reactions proceeded with the complete *para*-regioselectivity with respect to the phenyl group to afford the products 9–15.

Some of the primary substitution products were subsequently transformed, viz. fluoroalkyl sulfide **13** was oxidized to the corresponding sulfoxide **16**, while (3-aminopropyl)amino derivative **15** was bis-fluoroalkylated at the primary amino group to afford dendrimeric **19**. The experience in modification reactions of **1a** was successfully applied to *meso*-5,10,15,20-tetrakis(pentafluorophenyl)porphyrin (**20**) as reported recently [8] and in reactions with semi-protected propane-1,3-diamine (products **20** and **21**).

DFT calculations of the attack of model nucleophiles, ammonia, fluoride and hydroxide anion were successfully accomplished and based on the respective transition state energies confirmed the experimentally observed regioselectivity. Compared to the previously used naked fluoride anion, microsolvated LiF and LiOH as the model nucleophiles led to more realistic description of the model chemistry.

Based on the computational analysis, the regioselectivity can be attributed to higher polarizability of the system during the C-4 attack and improved stability of the corresponding dearomatized transition states, which corresponds well with their lower HOMO orbital energy. No Meisenheimer-type intermediates were formed in the course of the simulated reactions; instead, a tetrahedral S_N2 mechanism was found.

5. Experimental

5.1. General

Temperature data are uncorrected. Commercially available starting materials, reagents and solvents were used without further purification unless otherwise stated. THF was dried by sodium benzophenone ketyl and distilled prior to use. Column chromatography was performed on silica gel (63–200 μm, Merck). All reactions were carried out under nitrogen and reaction mixtures were stirred (magnetic spinbar). Apparatus were dried in oven and cooled under nitrogen. NMR spectra were recorded on a Bruker 400 AM (^{19}F at 376.6 Hz) and Varian Gemini 300 HC (^{1}H at 300.07 Hz, ^{13}C at 75.46 Hz) instruments: TMS and $CFCl_3$ as the internal standards, chemical shifts δ in ppm, coupling constants J (Hz), solvents $CDCl_3$ or CD_3OD. Mass spectra were scanned on a Hewlett Packard MSD 5971A (EI 70 eV) and MALDI-TOF Biflex IV (Bruker Daltonics) instruments.

5.2. Computations

DFT calculations were performed using Gaussian 03W program suite [25]. MP2 and IRC calculations were accomplished with Firefly QC package [26], which is partially based on the GAMESS (US) source code [27]. Vibrational frequencies were calculated for all species to characterise them as minima or transition states. Transition states geometries were found starting from the corresponding minima on the potential energy surfaces and estimated transition states using Schlegel's QST2 or QST3 method [28]. In all cases, the connections of the corresponding transition states and minima were verified by IRC calculations of the simulated reaction pathways. Vizualizations of the molecules were performed with the GaussView program [29].

5.3. The chemicals prepared and obtained

3,3,4,4,5,5,6,6,7,7,8,8,8-Tridecafluorooctan-1-ol (Atofina – Elf Atochem); 1,2;3,4-di-*O*-isopropylidene-D-xylitol (**4**) was prepared according to Refs. [30a,b]; allyl thiol (**5**) was prepared from allyl mercaptane and thiourea according to Ref. [30c] in 85% yield. 3,3,4,4,5,5,6,6,7,7,8,8,9,9,10,10,10-Heptadecafluorodecane-1-thiol (**6**) was prepared from 3,3,4,4,5,5,6,6,7,7,8,8,9,9,10,10,10-heptadecafluoro-1-iododecane and thiourea according to Ref. [30d] in 44% yield. *tert*-Butyl-*N*-(3-aminopropyl)carbamate (**7**) was prepared from di-*tert*-butyl dicarbonate and propane-1,3-diamine in 98% yield using a modified procedure [30e]. 2-(3,3,4,4,5,5,6,6,7,7,8,8,8-Tridecafluoroheptyl)-oxirane was prepared from tridecafluorohexyl iodide (Atofina – Elf Atochem) according to Ref. [30f].

5.4. 2,3,5,6-Tetrafluoro-4-(2,2,2-trifluoroethoxy)biphenyl (9)

A mixture of PFBi (**1a**, 50 mg, 0.205 mmol), 2,2,2-trifluoroethanol (**2**, 2 mL, 2.74 g, 27.4 mmol), K_2CO_3 (42 mg, 0.305 mmol) and dioxane (5 mL) was refluxed for 3 days. The solvent was removed under reduced pressure (rotary evaporator) and the crude product was purified by column chromatography (hexane) and crystallised (hexane). Product **9** (66 mg, 97%) as white crystals, m.p. 103–104 °C. ^{1}H NMR ($CDCl_3$):δ = 4.57 (q, $^3J_{HF}$ = 8 Hz, 2 H, CH_2,), 7.45 (m, 5 H, Ar) ppm. ^{19}F NMR ($CDCl_3$): δ = −75.4 (t, $^3J_{H,F}$ = 8 Hz, 3 F), −144.4 (dd, $^3J_{F,F}$ = 17.6 Hz, $^5J_{F,F}$ = 9.1 Hz, 2 F), −157.4 (dd, $^3J_{F,F}$ = 17.7 Hz, $^5J_{F,F}$ = 8.9 Hz, 2 F) ppm. ^{13}C NMR ($CDCl_3$): δ = 70.5 (q, $^2J_{C,F}$ = 36 Hz, CH_2), 122.7 (q, $^1J_{C,F}$ = 277 Hz, CF_3), 128.7, 129.2, 130.1 (3x s, Ar–H), 126.8 (s, Ar–H), 145.8, 142.6, 139.5, 136.3 (4x m, Ar–F) ppm. MS (EI, M_r = 324), m/z = 325 (10) [M^++1], 255 (71), 233 (19), 135 (100).

5.5. 2,3,5,6-Tetrafluoro-4-(3,3,4,4,5,5,6,6,7,7,8,8,8-tridecafluoroctan-1-yloxy)biphenyl (10)

A solution of 3,3,4,4,5,5,6,6,7,7,8,8,8-tridecafluorooctan-1-ol (196 mg, 0.45 mmol) in THF (2 mL) was added dropwise to a mixture of NaH (60%, 17 mg, 0.41 mmol) and THF (2 mL) while stirring. The reaction mixture was then stirred at r.t for 0.5 h and at 40 °C 0.5 h. A solution of PFBi (**1a**, 100 mg, 0.41 mmol) in THF (2 mL) and added dropwise to the solution of the sodium alkoxide **3** and the mixture was stirred at 80 °C for 2 days. The solvent was removed under reduced pressure (rotary evaporator) and the crude product was purified by column chromatography (hexane) and crystallised (hexane). Product **10** (102 mg, 38%) as white crystals, m.p. 84–86 °C. ^{1}H NMR ($CDCl_3$): δ = 2.70 (m, 2 H, CH_2–R_F), 3.75 (m, 2 H, CH_2–O–Ar), 7.44 (m, 5 H, Ar) ppm. ^{19}F NMR ($CDCl_3$): δ = −81.3 (t, $^3J_{F,F}$ = 10 Hz, 3 F, CF_3), −113.8 (m, 2 F, CF_2–CH_2), −122.4 (m, 2 F, CF_2), −123.3 (m, 2 F, CF_2), −124.0 (m, 2 F, CF_2), −126.6 (m, 2 F, CF_2), −144.9 (dd, $^3J_{F,F}$ = 22.2 Hz, $^5J_{F,F}$ = 8.8 Hz, 2 F), −157.7 (dd, $^3J_{F,F}$ = 22.3 Hz, $^5J_{F,F}$ = 8.8 Hz, 2 F) ppm. $C_{20}H_9F_{17}O$ (588.3): calcd. C 40.8, H 1.54; found C 40.9, H 1.68.

5.6. 1,2;3,4-Di-O-4-isopropylidene-5-O-(2,3,5,6-tetrafluorobiphenyl-4-yl)-D-xylitol (11)

Diisopropylidenexylitol **4** (105 mg, 0.45 mmol) in THF (2 mL) was added dropwise to a mixture of NaH (60%, 17 mg, 0.41 mmol) and THF (2 mL). The reaction mixture was refluxed for 2.5 h. A solution of PFBi (**1a**, 100 mg, 0.41 mmol) in THF (2 mL) was added dropwise to the reaction mixture, which was then refluxed at r.t. for 2 days. The solvent was removed under reduced pressure (rotary evaporator) and the crude product was purified by column chromatography (hexane–acetone, 7:1) and crystallised (hexane). The yield of **11** was 111 mg (60%) as white crystals, m.p. 94–96 °C. ^{1}H NMR ($CDCl_3$): δ = 1.41, 1.46, 1.49 (3 × s, 12 H, 4x CH_3), 3.95, 4.14, 4.3, 4.4, 4.41 (5 × m, 7 H, xylitol), 7.44 (m, 5 H, Ar) ppm. ^{19}F NMR ($CDCl_3$): δ = −145.3 (dd, $^3J_{F,F}$ = 22.3 Hz, $^5J_{F,F}$ = 8.8 Hz, 2 F,), −157.5 (dd, $^3J_{F,F}$ = 22.3 Hz, $^5J_{F,F}$ = 8.8 Hz, 2 F) ppm. $C_{23}H_{24}F_4O_5$ (456,4): calcd. C 60.6, H 5.34; found C 60.6, H 5.22.

5.7. 4-Allylsulfanyl-2,3,5,6-tetrafluorobiphenyl (12)

A mixture of PFBi (**1a**, 150 mg, 0.61 mmol), allylthiol (**5**, 45 mg, 0.61 mmol), K_2CO_3 (0.85 g, 0.61 mmol) and DMF (5 mL) was stirred at 40 °C for 2 h. The solvent was removed under reduced pressure (rotary evaporator) and crude product was purified by column chromatography (hexane) and crystallised (hexane). Product **12** (172 mg, 96%) as white crystals, m.p. 72–73 °C. ^{1}H NMR ($CDCl_3$): δ = 3.58 (d, $^3J_{H,H}$ = 7.2 Hz, 2 H, CH_2–S–Ar), 5.05 (dd, $^3J_{H,H}$ = 9.6 Hz, $^2J_{H,H}$ = 1.3 Hz, 1 H, CH = CH_2, H_{cis}), 5.06 (dd, $^3J_{H,H}$ = 16.8 Hz, $^2J_{H,H}$ = 1.3 Hz, 1 H, CH = CH_2, H_{trans}), 5.83 (ddt, $^3J_{H,H}$ = 9.6 Hz, $^3J_{H,H}$ = 16.8 Hz, $^3J_{H,H}$ = 7.2 Hz, 1 H, CH = CH_2), 7.46 (m, 5 H, Ar) ppm. ^{19}F NMR ($CDCl_3$): δ = −134.4 (dd, $^3J_{F,F}$ = 24 Hz, $^5J_{F,F}$ = 12 Hz, 2 F), −144.3 (dd, $^3J_{F,F}$ = 24 Hz, $^5J_{F,F}$ = 12 Hz, 2 F) ppm. $C_{15}H_{10}F_4S$ (298.3): calcd. C 60.4, H 3.38; found C 60.4, H, 3.54.

5.8. 2,3,5,6-Tetrafluoro-4-[(3,3,4,4,5,5,6,6,7,7,8,8, 9,9,10,10,10-heptadecafluorodec-1-yl)sulfanyl]biphenyl (13)

A mixture of PFBi (**1a**, 50 mg, 0.205 mmol), thiol **6** (99 mg, 0.205 mmol), K_2CO_3 (28 mg, 0.205 mmol) and DMF (5 mL) was stirred at 50 °C for 2 h. The solvent was removed under reduced pressure (rotary evaporator) and crude product was purified by column chromatography (hexane) and crystallised (hexane). Product **13** (133 mg, 92%) as white crystals, m.p. 108–109 °C. ^{1}H NMR ($CDCl_3$): δ = 2.46 (m, 2 H, CH_2–R_F), 3.18 (m, 2 H, CH_2–S–Ar), 7.44 (m, 5 H, Ar) ppm. ^{19}F NMR ($CDCl_3$): δ = −80.9 (t, $^3J_{F,F}$ = 10 Hz, 3 F, CF_3), −113.9 (m, 2 F, CF_2–CH_2), −121.7 (m, 6 F, 2 × CF_2), −122.5 (qs, 2 F, CF_2), −123.0 (qs, 2 F, CF_2), −125.9 (qs, 2 F, CF_2), −133.7 (dd, $^3J_{F,F}$ = 23.2 Hz, $^5J_{F,F}$ = 11 Hz, 2 F), −142.1 (dd, $^3J_{F,F}$ = 24 Hz, $^5J_{F,F}$ = 11 Hz, 2 F) ppm. ^{13}C NMR ($CDCl_3$): δ = 25.7 (s, SCH_2), 32.5 (t, $^2J_{C,F}$ = 22.3 Hz, CH_2R_F), 107.6–122.0 (m, 7 × CF_2, CF_3), 127.0 (s, Ar–H), 128.7, 129.48, 130.1 (3 × s, Ar–H), 142.7, 145.3, 146.1, 148.5 (4 × m, Ar–F) ppm. $C_{22}H_9F_{21}S$ (704.4): calcd. C 37.5, H 1.29; found C 37.3, H 1.46.

5.9. 3-[N-(2,3,5,6-Tetrafluorobiphenyl-4-yl)amino]propan-1-ol (14)

A mixture of PFBi (**1a**, 62 mg, 0.254 mmol), 3-aminopropan-1-ol (**7**, 19 mg, 0.254 mmol), K_2CO_3 (35 mg, 0.254 mmol) and dioxane (5 mL) was refluxed for 2 weeks. The solvent was removed under reduced pressure (rotary evaporator) and crude product was purified by column chromatography (CH_2Cl_2) and crystallised (hexane). Product **14** (73 mg, 60%) as white crystals, m.p. 68–70 °C. ^{1}H NMR ($CDCl_3$): δ = 1.90 (qi, $^3J_{H,H}$ = 6 Hz, 2 H, $CH_2CH_2CH_2$), 3.59 (tt, $^3J_{H,H}$ = 6.6 Hz, $^5J_{F,H}$ = 1.65 Hz, 2 H, CH_2NH), 3.84 (t, $^3J_{H,H}$ = 6.1 Hz, 2 H, CH_2OH), 7.45 (m, 5 H, Ar) ppm. ^{19}F NMR ($CDCl_3$): δ = −147.2 (d, $^3J_{F,F}$ = 14 Hz, 2 F), −157.4 (d, $^3J_{F,F}$ = 14.4 Hz, 2 F,) ppm. ^{13}C NMR ($CDCl_3$): δ = 32.8 (s, $CH_2CH_2CH_2$), 43.8 (t, $^4J_{C,F}$ = 4 Hz, ArNHCH_2), 61.1 (s, CH_2OH), 127.2 (t, $^3J_{C,F}$ = 12 Hz, Ar–H), 128.2, 128.4, 130.6 (3 × s, Ar–H), 136.1, 139.4, 142.80, 146.0 (4 × m, Ar–F), 156.4 (s, C═O) ppm. MS (EI, M_r = 299): m/z = 298 (100) [M^+−1], 281 (25), 255 (88), 241 (38), 227 (38), 207 (13).

5.10. tert-Butyl N-{3-[N-(2,3,5,6-tetrafluorobiphenyl-4-yl)amino]propyl} carbamate (15)

A mixture of PFBi (**1a**, 332 mg, 1.36 mmol), carbamate **8** (317 mg, 1.84 mmol), K_2CO_3 (188 mg, 1.36 mmol) and dioxane (5 mL) was refluxed for 2 weeks. The solvent was removed under reduced pressure (rotary evaporator) and crude product was twice

purified by column chromatography (hexane and hexane – CH_2Cl_2, 1:1) and crystallised (hexane). Product **15** (402 mg, 74%) as white crystals, m.p. 126–127 °C. ^{1}H NMR ($CDCl_3$): δ = 1.46 (s, 9 H, CH_3), 1.77 (qi, $^3J_{H,H}$ = 6.6 Hz, 2 H, $CH_2CH_2CH_2$), 3.27 (q, $^3J_{H,H}$ = 6.6 Hz, 2 H, OCONHCH_2), 3.47 (q, $^3J_{H,H}$ = 6 Hz, 2 H, ArNHCH_2CH$_2$), 4.42, 4.64 (2 × broad s, 2 H, 2 × NH), 7.45 (m, 5 H, Ar) ppm. ^{19}F NMR ($CDCl_3$): δ = −147.2 (d, $^3J_{F,F}$ = 14.8 Hz, 2 F), −160.8 (d, $^3J_{F,F}$ = 14 Hz, 2 F) ppm. ^{13}C NMR ($CDCl_3$): δ = 28.4 (s, CH_3), 31.3 (s, $CH_2CH_2CH_2$), 37.4 (s, ArNHCH_2), 42.8 (s, OCONHCH_2), 79.5 (s, O-C), 127.0 (s, Ar–H), 128.2, 128.4, 130.3 (3 × s, Ar–H), 136.3, 139.5, 142.8, 146.2 (4 × m, Ar–F), 156.4 (s, C = O) ppm. MS (EI, M_r = 398): m/z = 397 (35) [M^+−1], 323 (42), 265 (12), 233 (33), 156 (72), 133 (100). $C_{20}H_{22}F_4N_2O_2$ (398.4): calcd. C 60.3, H 5.57, N 6.93; found C 60.3, H 5.64, N 7.04.

5.11. 2,3,5,6-Tetrafluorobiphenyl-4-yl (3,3,4,4,5,5,6,6,7,7,8,8,8,9,9,10,10,10-heptadecafluorodec-1-yl) sulfoxide (16)

Dry flask was charged under nitrogen with CH_2Cl_2 (2 mL), trifluoroacetic acid (5 mL) and sulfide **13** (50 mg, 0.071 mmol). The solution was cooled to 0 °C, diluted H_2O_2 was then dropwise added (30%, 0.1 mL) and the mixture stirred for 1 h. The mixture was evaporated to dryness and crude product purified by column chromatography (hexane) to get pure **16** (42 mg, 82%) as white crystals, m.p. 121–122 °C. ^{1}H NMR (CDCl $_3$): δ = 2.74 (m, 2 H, CH_2–R_F), 3.4 (m, 1 H, CH_2–S(O)–Ar), 3.78 (m, 1H, CH_2–S(O)–Ar), 7.5 (m, 5 H, Ar) ppm. ^{19}F NMR ($CDCl_3$): δ = −81.2 (t, $^3J_{F,F}$ = 10 Hz, 3 F, CF_3), −113.7 (m, 2 F, CF_2–CH_2), −122.1 (m, 2 F, CF_2), −122.4 (m, 4 F, 2 × CF_2), −123.2 (m, 2 F, CF_2), −123.5 (m, 2 F, CF_2), −126.6 (m, 2 F, CF_2), −140.5 (m, 4 F, Ar) ppm. ^{13}C NMR ($CDCl_3$): δ = 45.3 (s, S(O)CH_2), 25.5 (t, $^2J_{C,F}$ = 22.4 Hz, CH_2R_F), 107.6–122.0 (m, 7 × CF_2, CF_3), 126.1 (s, Ar–H), 128.9, 129.9, 130.1 (3 × s, Ar–H), 142.7, 145.3, 145.3, 146.1, 148.5 (4 × m, Ar–F) ppm. MS (MALDI, M_r = 720,35): m/z = 721.19 [M^++1].

5.12. 3-[N-(2,3,5,6-Tetrafluorobiphenyl-4-yl)amino]propylammonium chloride (17)

Dry gaseous HCl was introduced into the solution of carbamate **15** (100 mg, 0.251 mmol) of Et_2O (15 mL) for 1 h. The mixture was evaporated to dryness (rotary evaporator, 40 °C, 20 mmHg) and then dried on oil pump for 5 h to afford product **17** (83 mg, 98%) as white crystals, m.p. 205–207 °C. ^{1}H NMR (CD_3OD): δ = 1.97 (qi, $^3J_{H,H}$ = 7.1 Hz, 2 H, $CH_2CH_2CH_2$), 3.04 (t, $^3J_{H,H}$ = 7.7 Hz, 2 H, CH_2NH$_2$·HCl), 3.51 (t, $^3J_{H,H}$ = 6.6 Hz, 2 H, ArNHCH_2CH$_2$), 7.4 (m, 5 H, Ar) ppm. ^{19}F NMR (CD_3OD): δ = −147.5 (d, $^3J_{F,F}$ = 14 Hz, 2 F), −161.0 (d, $^3J_{F,F}$ = 14 Hz, 2 F) ppm. ^{13}C NMR (CD_3OD): δ = 30.2 (s, $CH_2CH_2CH_2$), 38.7 (s, ArNHCH_2), 43.5 (s, CH_2NH$_2$·HCl), 127.02 (s, Ar–H), 129.4, 129.5, 131.4 (3 × s, Ar–H), 137.4, 140.6, 144.2, 147.3 (4 × m, Ar–F) ppm. MS (EI, M_r = 335): m/z = 299 (75) [M^++ 1–HCl], 282 (35), 254 (100), 234 (8).

5.13. N-{3-[N-(2,3,5,6-tetrafluorobiphenyl-4-yl)amino]propyl}-2,2,3,3,4,4,5,5,6,6,7,7,8,8,8-pentadecafluoroctanamide (18)

Dry flask (25 mL) was charged with amine hydrochloride 17 (25 mg, 0.107 mmol) and CH_2Cl_2 (10 mL) through septum. The solution was cooled to 0 °C and a solution of perfluorooctanoyl chloride (92 mg, 0.212 mmol) in CH_2Cl_2 (3 mL) and then a solution of triethylamine (32 mg, 0.317 mmol) in CH_2Cl_2 (3 mL) were added dropwise while stirring. The mixture was stirred at 0 °C for 2 h to become homogeneous and then evaporated to dryness (rotary evaporator, 40 °C, 650 mmHg). The solid residue was dissolved in Et_2O (15 mL), washed with saturated water solution of $KHCO_3$ (3× 25 mL), then with saturated water solution of NaCl (3× 25 mL) and the organic layer dried over $MgSO_4$. After removing the solvent, the residue was chromatographed (petroleum ether–dichloromethane, 1:1). Product 18 (53 mg, 72%) as white crystals, m.p. 119–121 °C. ^{1}H NMR ($CDCl_3$): δ = 1.92 (qi, $^3J_{H,H}$ = 6.6 Hz, 2 H, $CH_2CH_2CH_2$), 3.58, 3.51 (2 × q, $^3J_{H,H}$ = 6.6 Hz, 4 H, NHCH_2), 4.11 (broad s, ArNH), 6.64 (broad s, NHCO), 7.4 (m, 5 H, Ar) ppm. ^{19}F NMR ($CDCl_3$): δ = −81.2 (t, $^3J_{F,F}$ = 10 Hz, 3 F, CF_3) −119.8 (t, $^3J_{F,F}$ = 12.8 Hz, 2 F, CF_2CO), −122.0 (m, 2 F, CF_2), −122.4 (m, 2 F, CF_2), −122.9 (m, 2 F, CF_2), −123.2 (m, 2 F, CF_2), −126.6 (m, 2 F, CF_2), −146.9 (d, $^3J_{F,F}$ = 13.7 Hz, 2 F, Ar), −160.8 (d, $^3J_{F,F}$ = 14.9 Hz, 2 F, Ar) ppm. ^{13}C NMR ($CDCl_3$): δ = 29.7 (s, $CH_2CH_2CH_2$), 37.6 (s, ArNHCH_2), 43.0 (s, CONHCH_2), 106.9–118.3 (m, 6x CF_2, CF_3), 126.5 (t, $^3J_{C,F}$ = 11.5 Hz, Ar–H), 158.1 (t, $^2J_{F,F}$ = 26 Hz, C=O), 128.0 (s, Ar–H), 128.3, 128.5, 130.2 (3 × s, Ar–H), 136.9, 138.9, 143.5, 145.4 (4 × m, Ar–F) ppm. $C_{23}H_{13}F_{19}N_2O$ (694.3): calcd. C 39.8, H 1.89, N 4.03; found C 39.4, H 2.12, N 3.91.

5.14. N-{3-[N-(2,3,5,6-Tetrafluorobiphenyl-4-yl)amino]propyl}-1,1′-nitrilobis-(4,4,5,5,6,6,7,7,8,8,9,9,9,9-tridecafluorononan-2-ol) (19)

A mixture of amine hydrochloride **17** (20 mg, 0.085 mmol), fluoroalkyloxirane (Scheme 1, 300 mg, 0.798 mmol), triethylamine (9 mg, 0.089 mmol) and 2,2,2-trifluoroethanol (1 mL) was heated at 60 °C for 2 days while stirring. Volatile components were then removed (rotary evaporator, 45 °C, 50 mmHg) and the residue was chromatographed (petroleum ether–dichloromethane, 4:1) Product **19** (41 mg, 51%) as waxy material. ^{1}H NMR ($CDCl_3$): δ = 1.83 (m, 2 H, $CH_2CH_2CH_2$), 2.12–2.40 (m, 4 H, CH_2–R_F), 2.59–2.80 (m, 6 H, CH_2N), 3.50 (m, 4 H, NHCH_2, 2 × CH–OH), 4.21 (m, 3 H, ArNH, 2 × OH), 7.40 (m, 5H, Ar) ppm. ^{19}F NMR (CD_3Cl): δ = −81.4 (t, $^3J_{F,F}$ = 9.4 Hz, CF_3), −112.9 (qs, 2 F, CF_2–CH_2), −122.3 (qs, 2 F, CF_2), −123.4 (qs, 2 F, CF_2), −124.1 (qs, 2 F, CF_2), −126.7 (qs, 2 F, CF_2), −147.0 (dd, $^3J_{F,F}$ =14.3 Hz, $^5J_{F,F}$ = 6.4 Hz, 2 F), −161.0 (d, $^3J_{F,F}$ = 18.2 Hz, 2 F) ppm. ^{13}C NMR ($CDCl_3$): δ = 29.7 (s, $CH_2CH_2CH_2$), 37.0 (s, ArNHCH_2), 44.0 (m, CH_2–R_F), 53.4 (s, CH_2CH_2N), 60.5 (s, NCH_2CH(OH)), 63.9 (s, CH–OH), 107.6–121.5 (m, 12 C, 10 × CF_2, 2 × CF_3), 127.2 (m, Ar–H), 128.3, 128.42, 130.3 (3 × s, Ar–H), 136.6, 139.0, 143.3, 145.7 (4 × m, Ar–F) ppm. MS (MALDI, M_r = 1050,52): m/z = 1051.43 [M^++1].

5.15. 5,10,15-Tris(4-{[3-(tert-butoxycarbonyl)amino]propylamino}-2,3,5,6-tetrafluorophenyl)-20-(2,3,4,5,6-pentafluorophenyl)-21H,23H-porphyrin (21) and 5,10,15,20-tetrakis(4-{[3-(tert-butoxycarbonyl)-amino]propylamino}-2,3,5,6-tetrafluorophenyl)-21H, 23H-porphyrin (22).

A mixture of 5,10,15,20-tetrakis(pentafluorophenyl)porphyrin (**20**, 250 mg, 0.257 mmol), (3-amino-propyl)carbamate **8** (194 mg, 1.129 mmol), K_2CO_3 (156 mg, 1.129 mmol) and dioxane (6 mL) was heated at 100 °C for 3 weeks while stirring. After that time, TLC (hexane – acetone – CH_2Cl_2, 6:2:1) indicated only 2 products. The solvent was removed (rotary evaporator, 45 °C, 100 mmHg) and the residue chromatographed (solvent as for TLC) to afford tris-substituted product **21** (113 mg, 31%), m.p. 98–100 °C, and tetrakis-substituted product **22** (122 mg, 30%), m.p. 104–107 °C.

21: ^{1}H NMR ($CDCl_3$): δ = 9.03 (d, $^3J_{H,H}$ = 4.5 Hz, 2 H, (-H), 9,01 (s, 4 H, (-H), 8.87 (d, $^3J_{H,H}$ = 4.5 Hz, 2 H, β-H), 4.79 (t, $^3J_{H,H}$ = 6 Hz, 6 H, 6 × NH), 3.74 (t, $^3J_{H,H}$ = 6.6 Hz, 6 H, ArNHCH_2CH$_2$), 3.44 (qa, $^3J_{H,H}$ = 5.5 Hz, 6 H, OCONHCH_2), 1.97 (qi, $^3J_{H,H}$ = 6.6 Hz, 6 H, $CH_2CH_2CH_2$), 1.53 (s, 27 H, CH_3), −2.83 (s, 2 H, NH) ppm. ^{19}F NMR ($CDCl_3$): δ = −137.0 (d, $^3J_{F,F}$ = 21.5 Hz, 6 F), −161.3 (d, $^3J_{F,F}$ = 19.7 Hz, 6 F), −141.1 (m, 2 F, *ortho*), −152,8 (m, 1 F, *para*), −162,5 (m, 2 F, *meta*) ppm. ^{13}C NMR ($CDCl_3$, characteristic signals): δ = 160.1 (s, C=O), 79.65 (s, C–O), 42.9 (s, OCONHCH_2), 36.7 (s, ArNHCH_2), 31.6 (s, $CH_2CH_2CH_2$), 28.4 (s, CH_3) ppm. MS (FAB, M_r = 1437.28): m/z = 1437.2 [M^+].

22: ^{1}H NMR ($CDCl_3$): δ = 8.96 (s, 8 H, (-H), 4.83, 4.76 (2 × broad s, 8 × NH), 3.75 (qa, $^{3}J_{H,H}$ = 6.6 Hz, 8 H, ArNHCH_2CH$_2$), 3.44 (qa, $^{3}J_{H,H}$= 6.0 Hz, 8 H, OCONHCH_2), 1.99 (qi, $^{3}J_{H,H}$ = 6.6 Hz, 8 H, CH$_2$CH_2CH$_2$), 1.52 (s, 36 H, CH$_3$), −2.84 (s, 2 H, NH) ppm. ^{19}F NMR ($CDCl_3$): δ = −141.0 (d, $^{3}J_{F,F}$ = 17.8 Hz, 8 F), −161.3 (d, $^{3}J_{F,F}$ = 16.1 Hz, 8 F) ppm. ^{13}C NMR ($CDCl_3$): δ = 156.5 (s, C = O), 147.8, 145.9, 137.9, 136.1 (m, Ar$_F$), 129.1 (m), 104.8 (m), 79.5 (s, C-O), 42,9 (s, OCONHCH$_2$), 37.5 (s, ArNHCH$_2$), 31.5 (s, CH$_2$CH$_2$CH$_2$), 28.4 (s, 12 C, CH$_3$) ppm. MS (FAB, M_r = 1591.5): m/z = 1591.6 [M^+].

Acknowledgments

The authors thank the Atofina (Atochem) Company for the gift of perfluoroalkyl iodides. The research was supported by the Grant Agency of the Czech Republic (project No. 203/01/1311) and the Ministry of Education of the Czech Republic (project No. MSM 6046137301).

Appendix A. Supplementary data

Supplementary data associated with this article can be found, in the online version, at doi:10.1016/j.jfluchem.2010.09.003.

References

[1] (a) G. Chandra, A.D. Jenkins, M.F. Lappert, R.C. Srivastava, J. Chem. Soc. A (1970) 2550–2558;
(b) L.S. Kobrina, G.G. Furin, G.G. Yakobson, Zh. Org. Khim. 6 (1970) 512–520;
(c) L.N. Markovskii, G.G. Furin, Yu.G. Shermolovich, G.G. Yakobson, Izv. Akad. Nauk SSSR, Ser. Khim. (1981) 867–869;
(d) S. Fujii, Y. Maki, H. Kimoto, J. Fluorine Chem. 43 (1989) 131–144;
(e) V.M. Vlasov, I.A. Oskina, Russ. J. Org. Chem. 30 (1994) 1587–1592;
(f) J.H. Marriott, A.M.M. Barber, R.M. Grimshaw, S. Neidle, M. Jarman, J. Chem. Soc., Perkin Trans. 1 24 (2000) 4265–4278.
[2] (a) C. Tamborski, E.J. Soloski, J. Org. Chem. 31 (1966) 746–749;
(b) R. Filler, N.R. Ayangar, W. Gustowski, H.H. Kang, J. Org. Chem. 34 (1969) 534–538;
(c) V.M. Vlasov, O.V. Zakharova, Zh. Org. Khim. 11 (1975) 785–793.
[3] (a) R. Bolton, J.P.B. Sandall, J. Chem. Soc., Perkin Trans. 2 (1978) 746–750;
(b) R. Filler, R.C. Rickert, J. Fluorine Chem. 18 (1981) 483–496;
(c) V.M. Vlasov, G.G. Yakobson, Zh. Org. Khim. 17 (1981) 2192–2201;
(d) P.L. Coe, D. Oldfield, J.C. Tatlow, J. Fluorine Chem. 29 (1985) 341–348.
[4] (a) P.J.N. Brown, M.T. Chaudry, R. Stephens, J. Chem. Soc. C (1969) 2747–2750;
(b) D.M. Allen, A.S. Batsanov, G.M. Brooke, S.J. Lockett, J. Fluorine Chem. 108 (2001) 57–68.
[5] (a) M.T. Chaudry, R. Stephens, J. Chem. Soc. (1963) 4281–4283;
(b) D.G. Holland, J. Org. Chem. 29 (1964) 1562–1565;
(c) T.W. Lin, D.G. Naae, Tetrahedron Lett. (1978) 1653–1656.
[6] (a) P. Battioni, O. Brigaud, H. Desvaux, D. Mansuy, T.G. Traylor, Tetrahedron Lett. 32 (1991) 2893–2896;
(b) N. Jagerovic, A. Fruchier, J. Elguero, J. Heterocyclic Chem. 32 (1995) 1829–1831;
(c) P. Battioni, E. Cardin, M. Louloudi, B. Schölhorn, G.A. Spyroulias, D. Mansuy, T.G. Taylor, Chem. Commun. (1996) 2037–2038;
(d) D. Bouy-Debec, O. Brigaud, P. Leduc, P. Battioni, D. Mansuy, Gazz. Chim. Ital. 126 (1996) 233–237;
(e) A. Sen, K. Avijit, Tetrahedron Lett. 37 (1996) 5421–5424.
[7] (a) M. Suarez, E. Salfran, R.I. Curiel, F. Gaudemer, J. Elguero, Bull. Soc. Chim. Belg. 106 (1997) 323–326;
(b) R. Breslow, B. Gabriele, J. Yang, Tetrahedron Lett. 39 (1998) 2887–2890;
(c) S.J. Shaw, C. Edwards, R.W. Boyle, Tetrahedron Lett. 40 (1999) 7585–7586;
(d) S. Evans, J.R.L. Smith, J. Chem. Soc., Perkin Trans. 2 (2000) 1541–1551.
[8] (a) B. Dolenský, V. Král, in: Proceedings of the 24th International Symposium on Macrocyclic Chemistry, Barcelona PS2-15, 1999;
(b) M. Beneš, O. Paleta, V. Král, Chem. Listy 95 (2001) 743;
(c) K. Lang, V. Král, P. Kapusta, P. Kubát, P. Vašek, Tetrahedron Lett. 43 (2002) 4919–4922.
[9] (a) P. Pasetto, X. Chen, C.M. Drain, R.W. Franck, Chem. Commun. (2001) 81–82;
(b) R. Weiss, F. Pühlhofer, N. Jux, K. Merz, Angew. Chem. Int. Ed. 41 (2002) 3815–3817;
(c) J.P.C. Tomé, M.G.P.M.S. Neves, A.C. Tomé, J.A.S. Cavaleiro, A.F. Mendonca, I.N. Pegado, R. Duare, M.L. Valdeira, Bioorg. Med. Chem. 13 (2005) 3878–3888;
(d) D. Samaroo, C.E. Soll, L.J. Todaro, C.M. Drain, Org. Lett. 8 (2006) 4985–4988;
(e) P.S.S. Lacerda, A.M.G. Silva, A.C. Tomé, M.G.P.M.S. Neves, A.M.S. Silva, J.A.S. Cavaleiro, A.L. Llamas-Saiz, Angew. Chem. Int. Ed. 45 (2006) 5487–5491.
[10] (a) B.H. Lee, M.J. Miller, J. Org. Chem. 48 (1983) 24–31;
(b) A. Malabarba, R. Ciabatti, J. Kettenring, R. Scotti, G. Candiani, J. Med. Chem. 35 (1992) 4054–4060.
[11] B. Guyot, B. Ameduri, B. Boutevin, J. Fluorine Chem. 74 (1995) 233–240.
[12] (a) J. Burdon, Tetrahedron 21 (1965) 3373–3380;
(b) O. Paleta, Usp. Khim. 40 (1971) 855–917;
(c) R.D. Chambers, Fluorine in Organic Chemistry, A. Rowe, Chippenham, 1973, p. 283;
(d) G.M. Brooke, J. Fluorine Chem. 86 (1997) 1–76;
(e) R.D. Chambers, P.A. Martin, G. Sandford, D.L.H. Williams, J. Fluorine Chem. 129 (2008) 998–1002.
[13] (a) J. Shorter, in: N.B. Chapman, J. Shorter (Eds.), Advances in Linear Free Energy Relationships, Plenum Press, London, 1972, pp. 71–96;
(b) O. Exner, in: N.B. Chapman, J. Shorter (Eds.), Correlation Analysis in Chemistry—Recent Advances, Plenum Press, New York, 1978, pp. 439–467;
(c) O. Exner, Correlative Relationships in Organic Chemistry, SNTL, Prague, (1981), pp. 70–91.
[14] (a) P. Robson, M. Stacey, R. Stephens, J.C. Tatlow, J. Chem. Soc. (1960) 4754–4760;
(b) J. Burdon, P.L. Coe, C.R. Marsh, J.C. Tatlow, Tetrahedron 22 (1966) 1183–1188;
(c) M.E. Peach, A.M. Smith, J. Fluorine Chem. 4 (1974) 399–408.
[15] (a) J. Burdon, W.B. Hollyhead, J.C. Tatlow, J. Chem. Soc. (1965) 5152–5158;
(b) J.A. Godsell, M. Stacey, J.C. Tatlow, Nature 178 (1956) 199–200;
(c) W.J. Pummer, L.A. Wall, Nature 127 (1958) 643–644.
[16] (a) J.G. Allen, J. Burdon, J.C. Tatlow, J. Chem. Soc. (1965) 6329–6337;
(b) G.G. Yakobson, V.D. Shteingarts, G.G. Furin, N.N. Vorozhtsov, Zh. Obshch. Khim. 34 (1964) 3514–3519.
[17] M.N. Glukhovtsev, R.D. Bach, S. Laiter, J. Org. Chem. 62 (1997) 4036–4046.
[18] K. Tanaka, M. Deguchi, S. Iwata, J. Chem. Res. (S) (1999) 528–529.
[19] M. Muir, J. Baker, J. Fluorine Chem. 126 (2005) 727–738.
[20] C.P. Brock, D.G. Naae, N. Goodhand, T.A. Hamor, Acta Crystrallogr. B34 (1978) 3691–3696.
[21] C. Adamo, V. Barone, J. Chem. Phys. 110 (1999) 6158–6170.
[22] (a) A.D. Boese, J.M.L. Martin, J. Chem. Phys. 121 (2004) 3405–3416;
(b) J. Hajduch, O. Paleta, J. Kvíčala, G. Haufe, Eur. J. Org. Chem. (2007) 5101–5111.
[23] (a) M.T. Cancès, B. Mennucci, J. Tomasi, J. Chem. Phys. 107 (1997) 3032–3041;
(b) B. Mennucci, J. Tomasi, J. Chem. Phys. 106 (1997) 5151–5158;
(c) B. Mennucci, E. Cancès, J. Tomasi, J. Phys. Chem. B 101 (1997) 10506–10517;
(d) J. Tomasi, B. Mennucci, E. Cancès, J. Mol. Struct. (Theochem) 464 (1999) 211–226.
[24] (a) B.H. Besler, K.M. Merz Jr., P.A. Kollman, J. Comp. Chem. 11 (1990) 431–439;
(b) U.C. Singh, P.A. Kollman, J. Comp. Chem. 5 (1984) 129–145.
[25] M.J. Frisch, G.W. Trucks, H.B. Schlegel, G.E. Scuseria, M.A. Robb, J.R. Cheeseman, J.A. Montgomery Jr., T. Vreven, K.N. Kudin, J.C. Burant, J.M. Millam, S.S. Iyengar, J. Tomasi, V. Barone, B. Mennucci, M. Cossi, G. Scalmani, N. Rega, G.A. Petersson, H. Nakatsuji, M. Hada, M. Ehara, K. Toyota, R. Fukuda, J. Hasegawa, M. Ishida, T. Nakajima, Y. Honda, O. Kitao, H. Nakai, M. Klene, X. Li, J.E. Knox, H.P. Hratchian, J.B. Cross, V. Bakken, C. Adamo, J. Jaramillo, R. Gomperts, R.E. Stratmann, O. Yazyev, A.J. Austin, R. Cammi, C. Pomelli, J.W. Ochterski, P.Y. Ayala, K. Morokuma, G.A. Voth, P. Salvador, J.J. Dannenberg, V.G. Zakrzewski, S. Dapprich, A.D. Daniels, M.C. Strain, O. Farkas, D.K. Malick, A.D. Rabuck, K. Raghavachari, J.B. Foresman, J.V. Ortiz, Q. Cui, A.G. Baboul, S. Clifford, J. Cioslowski, B.B. Stefanov, G. Liu, A. Liashenko, P. Piskorz, I. Komaromi, R.L. Martin, D.J. Fox, T. Keith, M.A. Al-Laham, C.Y. Peng, A. Nanayakkara, M. Challacombe, P.M.W. Gill, B. Johnson, W. Chen, M.W. Wong, C. Gonzalez, J.A. Pople, Gaussian 03, Revision D.01, Gaussian, Inc., Wallingford, CT, 2004.
[26] A.A. Granovsky, Firefly version 7.1.G, www.http://classic.chem.msu.su/gran/firefly/index.html.
[27] M.W. Schmidt, K.K. Baldridge, J.A. Boatz, S.T. Elbert, M.S. Gordon, J.H. Jensen, S. Koseki, N. Matsunaga, K.A. Nguyen, S. Su, T.L. Windus, M. Dupuis, J.A. Montgomery, J. Comput. Chem. 14 (1993) 1347–1363.
[28] P.Y. Ayala, H.B. Schlegel, J. Chem. Phys. 107 (1997) 375–384.
[29] R. Dennington II, T. Keith, J. Millam, K. Eppinnett, W.L. Hovell, R. Gilliland, GaussView, Version 3.09, Semichem, Inc., Shawnee Mission, KS, 2003.
[30] (a) N. Baggett, K.W. Buck, A.B. Foster, R. Jefferis, B.H. Rees, J.M. Webber, J. Chem. Soc. (1965) 3382–3387;
(b) L. Zarif, J. Greiner, S. Pace, J.G. Riess, J. Med. Chem. 33 (1990) 1262–1269;
(c) B. Ambekar, Y. Sarvottam, Synth. Commun. 29 (1999) 3477–3486;
(d) J.D. Glennon, S. Hutchinson, S.J. Harris, A. Walker, M.A. McKervey, C.C. McSweeney, Anal. Chem. 69 (1997) 2207–2212;
(e) D. Muller, I. Zeltser, G. Bitan, C. Gilon, J. Org. Chem. 62 (1997) 411–416;
(f) V. Církva, B. Améduri, B. Boutevin, O. Paleta, J. Fluorine Chem. 83 (1997) 151–158.